Nature Environment and Pollution Technology
An International Quarterly Scientific Journal

p-ISSN: 0972-6268
e-ISSN: 2395-3454

Vol. 19 | No. 1 | pp. 57-70 | 2020

Original Research Paper | Open Access

A Novel Approach to Utilize Used Disposable Paper Cups for the Development of Adsorbent and its Application for the Malachite Green and Rhodamine-B Dyes Removal from Aqueous Solutions

Kshipra Shukla, Alka Verma, Lata Verma, Shalu Rawat and Jiwan Singh†
Department of Environmental Science, Babasaheb Bhimrao Ambedkar University, Lucknow-226025, India
†Corresponding author: Jiwan Singh

Nat. Env. & Poll. Tech.
Website: www.neptjournal.com
Received: 12-06-2019
Accepted: 23-07-2019

Key Words:
Malachite Green
Rhodamine-B
Adsorption
AC@PC adsorbent

ABSTRACT

This study focuses on the removal of organic dyes, such as Malachite Green (MG) and Rhodamine-B (Rh-B) from an aqueous solution with the help of a novel adsorbent (activated carbon) with magnetic property prepared by used disposal paper cups (AC@PC) at 500°C. The synthesized AC@PC adsorbent was characterized by using Fourier transform infrared spectroscopy (FTIR), X-ray diffraction (XRD), scanning electron microscopy (SEM), Energy dispersive X-ray spectroscopy (EDS) and point of zero charge (pHZPC). Adsorption of MG and Rh-B onto the AC@PC adsorbent from aqueous solution was investigated systematically. Langmuir, Freundlich and Temkin isotherms were also studied, however, it has been observed that Langmuir isotherm model was best fitted for both the dyes, which describe the adsorption behaviour at equilibrium. Pseudo-first and pseudo-second order kinetic model describe the rate of adsorption. Kinetic study explained that the process of adsorption followed the pseudo-second order model. Thermodynamic parameters such as enthalpy (ΔH°), entropy (ΔS°) and Gibb's free energy (ΔG°) were also studied and revealed that the adsorption of MG was endothermic, whereas adsorption of Rh-B was exothermic onto the AC@PC. The prepared adsorbent shows potentially high adsorption properties for both the dyes.

INTRODUCTION

India is facing very serious problem of solid waste disposal. The waste contributes to landfills and are post-consumer products that means those substances which cannot be recycled or reused any longer (Arumugam et al. 2015). Paper cup waste disposal is a major issue in terms of environment as it is mainly composed of paper with high strength that can be easily recycled but the inner layer is lined with thin film of polyethylene and make paper cups recycling very complicated (Arumugam et al. 2018). These disposable cups are widely used all over the world for serving tea, coffee, soft-drinks and for many other purposes. Generation of municipal solid waste in India is approximately 1,88,550 tonnes per day of which 35% by weight constitutes post-consumer waste that causes serious problems to the society and environment (Arumugam et al. 2018). Post-consumer waste can be elaborated as the waste generated by the end consumer (Arena et al. 2016). In India solid waste management is a very big task for the generated waste. The paper waste can be very effective for removal of pollutants from water when it converted into an adsorbent. Utilization of paper cup waste for the adsorption purpose can reduce the problem of disposable of paper cup waste.

The discharge of water from the industries may hold pollutants such as dyes, heavy metals into the aqueous solution that disrupt the ecosystem of aquatic animals and plants and also causes various health problems in human beings. Several industries, for example, cosmetics, plastics, textile, processing, rubber etc. uses different classes of dyes (Kono 2015). Dyes are growing to be a very challenging class of pollutants to the environment causing many health hazards (Ngulube et al. 2017). Dyes are mainly the chemical compounds or complex organic molecules that imparts colour to the surface or fabric when comes in contact (Yagub et al. 2014).

Many industries discharge effluent into water bodies containing highly coloured species with large amount of toxic substances that not only cause health related problems but also degrade the aesthetic values of water bodies (Kant 2012). About 10,000 dyes produced yearly of which 7.105 metric tons are available in market. Around 15% of dye materials are misplaced in effluent discharged from various manufacturing and processing operations in industrial activities (Gupta et al. 2012). The dye effluent from industries contain certain chemicals that could be lethal, carcinogenic or mutagenic to living organisms (Noel & Rajan 2014). Synthetic dyes are highly soluble in water and are the common pollutants that

pollute water and normally found in industrial wastewater in trace amount (Crini 2006).

MG is usually used for the dyeing of the cotton, leather, paper, silk and also in different industries such as manufacturing of paints and printing inks. It is persistent in environment and acutely toxic to many aquatic and terrestrial animals (Gupta et al. 2016). While, Rh-B dye is used in textile, printing industries and photographic industries and it is a xanthene dye. Rh-B causes many health problems such as irritation of the eye, skin, and respiratory tract. This dye is carcinogenic, and also causes developmental and reproductive toxicity (Bhattacharya et al. 2014).

Numerous chemicals, physical and biological techniques, comprising biosorption, ozonation, adsorption, coagulation, advance oxidation, liquid-liquid extraction and membrane filtration have been extensively used for dyes treatment from the wastewater (Pathania et al. 2017). Among all the techniques used adsorption is very efficient, cheapest and eco-friendly method as it gives the best results when used for dyes removal from aqueous medium (Yagub et al. 2014).

The waste paper cups used for the preparation of AC@PC adsorbent is used for the first time as an adsorbent for the removal of MG and Rh-B. The main objective of this work is to synthesize the low-cost adsorbent with magnetic properties from waste disposable paper cups and its application for removal of MG and Rh-B dye from an aqueous solution. The present study is focusing on the management of waste disposable cups as well as for the treatment of water pollutants.

MATERIALS AND METHODS

Materials

Rh-B dye ($C_{21}H_{31}ClN_2O_3$) and MG dye ($C_{23}H_{25}N_2Cl$) were obtained from Thermo Fisher Scientific India Pvt. Ltd. These dyes were used directly without any purification. Double distilled water was used to prepare the solution of these dyes. PCs were collected from canteen of Babasaheb Bhimrao Ambedkar University, Lucknow, (U.P.), India.

Preparation of AC@PC Novel Adsorbents

Collected waste PCs were washed to eliminate filths present on the surface and then dried in hot air oven. After that, these paper cups were cut into small pieces and dipped into hot water (temperature 60-70°C) for 3-4 hours and then the thin lining made up of polyethylene was separated from the paper part. Wet paper clumps were removed from hot water and again dried in hot air oven at 105°C for 24h. The dried material was grinded and sieved with 0.25 mm sieve. Then 30 g of grounded material was added to the $FeCl_3$ solution (15g $FeCl_3$ + 150 mL distilled water). The mixture was kept on magnetic stirrer (model no. 1MLH, REMI, India) and stirred for four hours. The material was then filtered and kept overnight in an oven for drying. After drying, the material was kept in muffle furnace (IMPACT, 11C 106B) at 500°C for two hours then the material was crushed by mortar pestle to change it into powder form and was washed with deionized water for 2-3 times, oven dried for overnight and then it was used for the adsorption study (Lunge et al. 2014).

Characterization

Surface morphological structure of AC@PC sample was examined using SEM (JSM-6490 LV, JEOL, Japan). For SEM analysis the sample was coated on a tacky carbon tape and then mounted on a stub into a sample holder. EDS done for the determination of elemental composition of AC@PC.

An infrared spectrum was recorded using Infrared Spectrometer (Nicolet^{TM} 6700, Thermo Scientific, USA) for the functional group determinations present on the surface of AC@PC. The sample were prepared mixing spectroscopy grade KBr with oven dried (at 105°C) sample in an agate mortar.

XRD (Powder Diffractometer PW3040/60, PaNanalytical Neitherland) was used for the analysis of crystalline structure of AC@PC. Scanning of sample was done at the rate of 2° min^{-1} from 10°-80°.

Zeta nanosizer (Nano-ZS90), was used for analysing the particle size and zeta potential of AC@PC. Zeta potential of AC@PC was done at different pH (2, 4, 6, 8 and 10).

The pH_{ZPC} of synthesized material (AC@PC) was determined by using 0.1 M NaCl solution with different pH (2, 4, 6, 8 and 10). These pH values were adjusted by using solutions of 0.1 N HCl and 0.1 N NaOH. A 20 mL NaCl solution and 0.2 g adsorbent were taken and left for 48 hrs after that the pH of solution was measured by a pH meter. The pH_{zpc} value was attained by plotting the graph of initial pH against final pH (Singh et al. 2016).

Batch Adsorption Studies

Batch adsorption experiment was performed with AC@PC for MG and Rh-B removal from an aqueous medium. Initial concentrations were prepared in the range of 5-30 mg/L by diluting standard solution of 1000 mg/L of MG and Rh-B dyes separately. Adsorption studies were performed at different temperatures 25°C, 35°C and 45°C. Different doses in g/L (0.5, 1, 1.5, 2, 3, 3.5 and 4) were taken to optimize the dose at which the maximum adsorption of dye occurs. The dose study revealed that the maximum adsorption was obtained

with the dose of 3 g/L. A fixed dose of AC@PC (3 g/L) was taken for further study. All experiments were conducted in duplicate with 100 mL of dye solution in a 250 mL conical flask at 100 rpm for 300 min.

The conical flasks having samples were taken out from orbital shaker at different interval of time (5, 15, 30, 60, 120, 180, 240 and 300 min). All experiments were performed at normal temperature of 25°C except temperature study conducted at 35°C and 45°C. All experiments were conducted at neutral pH except pH study (pH 4, 5, 6, 7, 8, 9 and 10). The pH of working solution was maintained by 0.1 M NaOH or HCl, solution pH was then measured by using pH meter (water analyser, 372, Systronic India Limited). After that the solution was filtered and analysed to determine the remaining concentration using UV-Vis spectrophotometer (Model No. 117, Systronic India Ltd.).

The amount of dye (MG and Rh-B) q_t (mg/g) adsorbed on AC@PC, was evaluated by following equation:

$$\text{Removal } \% = \frac{C_0 - C_e}{C_0} \times 100 \quad \ldots(1)$$

Where, C_0 is the initial concentration (mg/L) and C_e is the equilibrium concentration (mg/L).

The adsorption capacity of adsorbent at equilibrium was calculated by following equation (Ibrahim et al. 2019):

$$q_e = \frac{C_0 - C_e}{m} \times V \quad \ldots(2)$$

Where,

V = volume of dye solution (L)

m = mass of adsorbent (g)

RESULT AND DISCUSSION

Adsorbent Characterization

SEM and EDS analysis: Fig. 1 (a) shows that the adsorbent has an irregular porous surface with cuboid/pyramid shaped crystal structures which may be responsible for the adsorption of MG and Rh-B. The EDS (Fig. 1b) analysis is mainly done to identify the elemental composition of material. The EDS analysis of AC@PC adsorbent shows the presence of various elements. AC@PC containing highest carbon content with 72.01%. Iron and aluminium content were present in the material and it was confirmed by SEM-EDS analysis. The lower point of zero charge value of AC@PC was due to the presence of Fe on the surface of adsorbent which caused acidic property (Karunanayake et al. 2018).

FTIR spectroscopy: The Fig. 1(c) shows FTIR spectrum of AC@PC before and after adsorption, that shows the presence of several functional groups on adsorbents surface. Peak at 3339.67 cm^{-1} signifies -OH stretching that denotes the presence of hydroxyl or phenol groups and the peak at 2926.7 cm^{-1} denote $-CH_3$ and $-CH_2-$ in aliphatic compound. C=O stretch was also represented by peaks at 1713.1 cm^{-1} beside these groups, peaks at 1587.5 cm^{-1} indicates the presence of $-NH_2$ stretch, peak at 1235.4 cm^{-1} represents C-N in aromatic amines, peak at 545.99 cm^{-1} represents COO- group in carboxylic acid (Magdalane et al. 2017).

Fig. 1(c) also describes the FTIR spectrum after adsorption of MG dye, peak at 2926.7 cm^{-1} represents $-CH_3$ and $-CH_2-$ in aliphatic compound and this peak also present in after adsorption in case of both the dyes. C=C stretching in vinyl ethers represented by peak at 1619.3 cm^{-1} and peak 1305.5 cm^{-1} shows N=N-O in azoxy salts compound, peak at 773.03 cm^{-1} also appeared that attribute to C-O bond bending vibration (Sartape et al. 2017). The Fig. 1(c) also shows the FTIR stretches present on adsorbents surface after adsorption of Rh-B dye.

Spectrum of FTIR analysis of AC@PC after adsorption of Rh-B showed the presence of stretches at 1462.4 cm^{-1} that correspond to $-CH_3$ in aliphatic compounds, peaks at 1368.7 cm^{-1} represents in aliphatic nitro compound, however peak at 1164.6 cm^{-1} represents -C-OH group of alcohol, and peak at 1031.9 cm^{-1} represents CH_2- O-H stretching of primary alcohols.

A peak at 545.99 cm^{-1} which represents C-C=O stretching in carboxylic acid present on adsorbent before adsorption but after adsorption it was observed as the reduced peaks height and new peaks were identified as follows -C=C- and N=N-O stretch in case of MG and CH_2-O-H in case of Rh-B. FTIR results show that after adsorption of MG and Rh-B shows a new peak having C-O and $-CH_3$ in aliphatic compound, respectively.

X-ray diffraction analysis: Fig. 1 (d) represents the XRD pattern of AC@PC which is almost similar to the magnetite. There are five characteristic peaks were obtained for Fe_3O_4 ($2\theta = 33.84°, 36.23°, 49.4°, 54.73°$ and $63.0°$), having indices (220, 311, 400, 422 and 440) (Lunge et al. 2014). Appearance of narrower and sharper peaks indicates the crystalline nature of AC@PC.

Particle size analysis (PSA): The particle size of AC@PC was determined by using Zeta nanosizer (Nano-ZS90), after blending it in uniform mixture in ethyl alcohol at room temperature. Obtained result has been plotted in Fig. 2(a) that shows broad peak in between the range of 150-350 nm that means the particle of AC@PC are in micrometre. Large size of the particles might be due to the clumping of particles with each other.

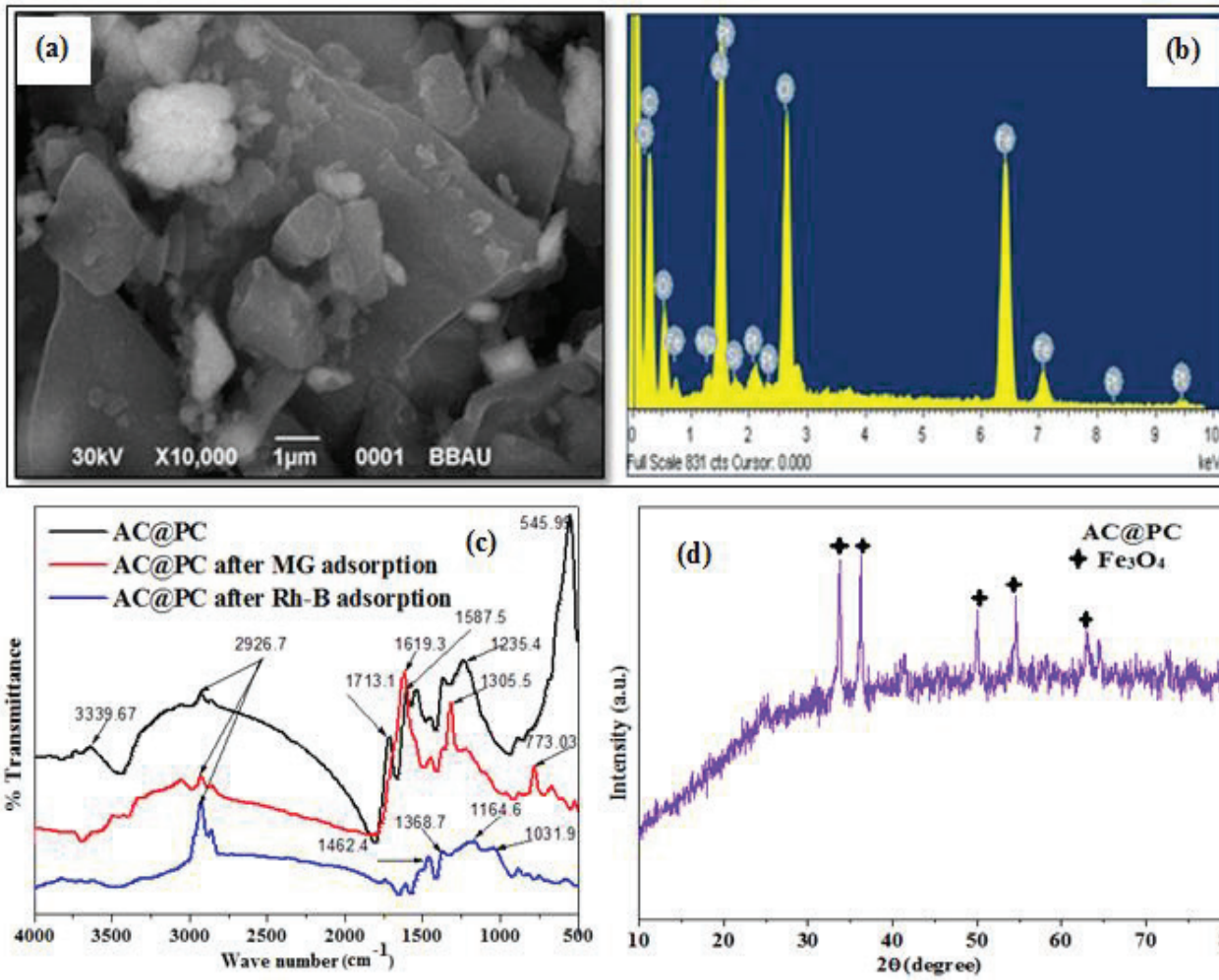

Fig. 1: Characterization (a) SEM and (b) EDS images of AC@PC, (c) FTIR spectrum of AC@PC before and after adsorption of dyes and (d) XRD image of AC@PC adsorbent.

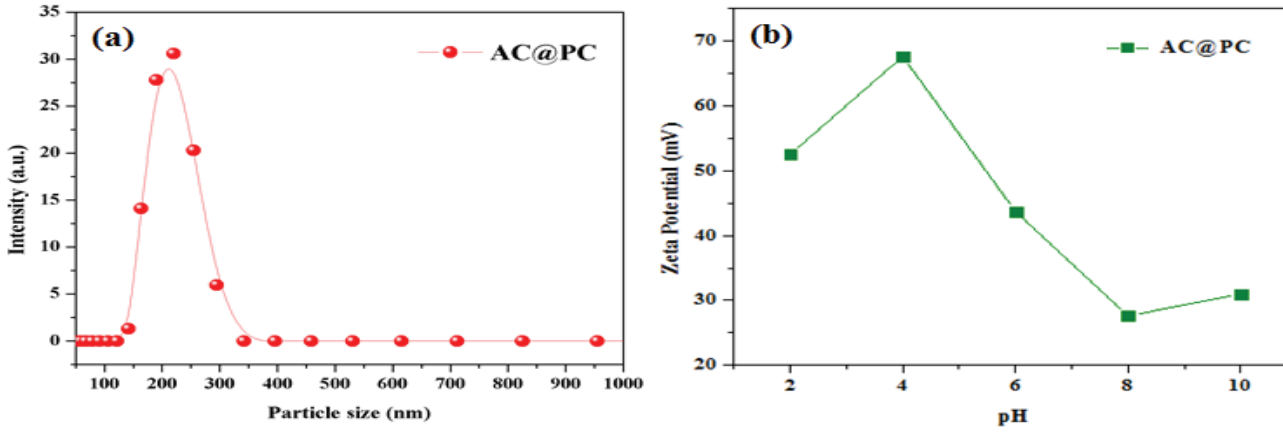

Fig. 2: (a) Particle size analysis and (b) Zeta potential of AC@PC.

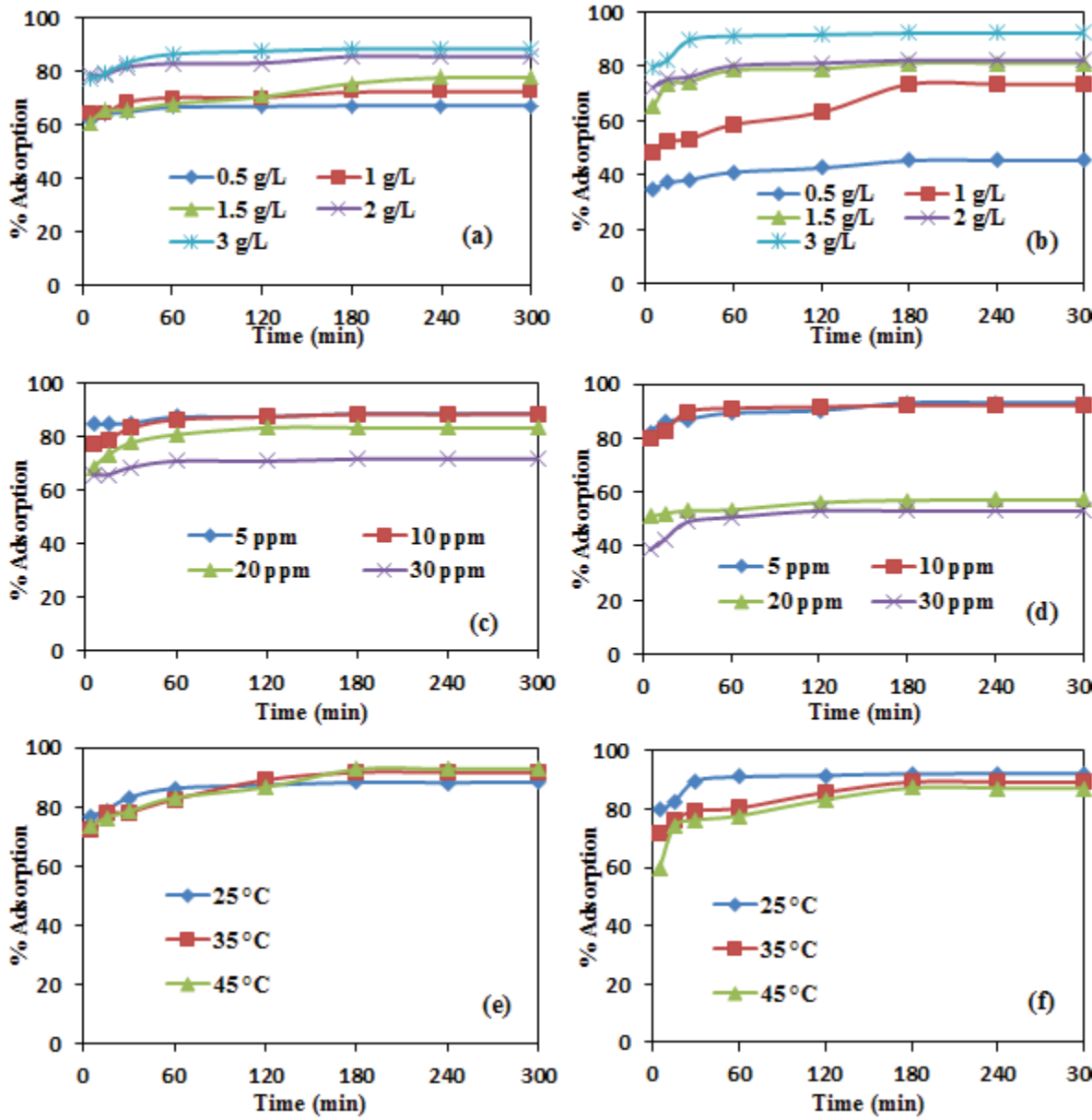

Fig. 3: Batch adsorption (a) and (b) Effect of dose, (c) and (d) effect of initial dye concentration, (e) and (f) effect of temperature for MG and Rh-B respectively.

Zeta potential: For the determination of zeta potential of synthesized AC@PC zeta nanosizer (Nano-ZS90), was used. The stability of adsorbent is identified by the magnitude of zeta potential in a dispersion medium. It works on the principle of electrostatic repulsion between the adsorbent and the dispersion medium (Gautam et al. 2018). The result obtained by zeta potential analysis at different pH is shown in Fig. 2(b). The adsorbent AC@PC was stable at acidic as well as at basic pH but highly stable at pH 2 (53.4 mV).

Point zero charge (pH_{ZPC}): Point zero charge determination of adsorbent is one of the very important characteristics to identify the pH value at which the adsorbent surface becomes neutral. The pHzpc of AC@PC was found to be 2.6. It means that the prepared material was acidic in nature and it may have ability to remove the cationic dyes. The high temperature (500°C) used in the AC@PC preparation process and $FeCl_3$ used to develop the magnetic properties in the material also imparts the acidic nature to the material.

Batch Adsorption Studies

Effect of dosage: Adsorbent dose is considered as a significant parameter of adsorption study, since it helps in determination of adsorbent capacity that how much amount of adsorbent could adsorb the maximum amount of initial concentration of dye, by varying amount of adsorbent while keeping other factors constant like, temperature, initial dye concentration, pH etc. Effect of adsorbent doses on the adsorption capacity was examined by taking different quantity of adsorbent dose in the range of (0.5, 1.0, 1.5, 2.0, 2.5 and 3.0 g/L) were added with an initial MG and Rh-B dyes initial concentration of 10 mg/L with contact time of 5-300 min at constant temperature of 25°C (298K) and neutral pH with shaking speed of 100 rpm. It was observed that on increasing dose from 0.5 g/L to 3 g/L, the removal percentages of both the dyes were increased. As shown in Fig. 3 (a) and (b), removal of MG and Rh-B was increased from 67.19 to 88.37% and 45.33 to 92.19%, respectively, when the amount of material increased from 0.5 to 3 g/L.

An increase in removal percentage of dyes on AC@PC happened due to the availability of adsorption sites on adsorbent surface, which provides more surface area for adsorption of dyes. Conversely, after a certain limit, increasing adsorbent concentration may cause agglomeration or overlapping of adsorbent sites, thus reducing the total surface area provided to dyes for adsorption (Gao et al. 2019).

Effect of concentration and contact time: In the adsorption study, initial dye concentration is very crucial parameter; removal percentage of dye is tremendously dependent on the amount of initial concentration of dye and also on the binding sites availability on the surface of adsorbent. The effect of initial concentration of dye (5 mg/L to 30 mg/L) and contact time was studied at 25°C (298K), the pH 7 with altering contact time (5-300 min). Fig. 3 (c) and (d) show that the removal percentages of MG and Rh-B were increased on increasing contact time from 5 to 300 min and decreases with increase in concentration of both the dyes. The removal percentage of MG was decreased from 88.43% to 71.64% while removal percentage of Rh-B was decreased from 93.08 % to 53.07 % on increasing initial dye concentration from 5 mg/L to 30 mg/L.

Usually the removal percentage of both dyes decreases as the initial concentration was increased which might be because of presence of limited adsorption sites and saturation of adsorbent (Salleh et al. 2011) and increase in initial dyes concentration, resulting an increase in adsorption capacity (Singh et al. 2015). The adsorbent having maximum adsorption capacity of 7.164 mg/g as shown in Fig. 4(c) for MG and 5.307 mg/g for Rh-B at 30 mg/L (Fig. 4e).

Effect of temperature on adsorption: The effect of temperature study was performed at various temperatures (25, 35 and 45°C) while retaining other experimental conditions constant such as dose of adsorbent (3 g/L), initial dyes concentration (10 mg/L) and pH 7 to check the effect of temperature on the rate of adsorption. Fig. 3(e) shows that the removal percentage was achieved about 88% at 25°C, however, when temperature increased up to 45°C, removal percentage was increased approximately 93% in case of MG and it shows the endothermic adsorption process, this might be due to the activation of some specific active sites on AC@PC surface and increasing mobility of dye molecules with increasing temperature (Yagub et al. 2014). On the other hand, Fig. 3(f) shows the exothermic adsorption of Rh-B i.e., removal percentage was decreased from 92.19% to 87.19% with an increase in temperature from 25 to 45°C. Exothermic process of adsorption might be because of adsorptive forces decreased between the active sites present on the surface of adsorbent and dye, while increasing temperature results in decrease in adsorption percentage (Salleh et al. 2011) or may be due to the dye molecules have a tendency to leave the solid phase and outflow to liquid phase at higher temperature (Nassar et al. 2016). In case of MG dye, it was observed that the adsorption was increased with increase in temperature and the maximum adsorption capacity was obtained as 3.093 mg/g at 45°C as shown in Fig. 4(d). Fig. 4(f) shows that the adsorption capacity of AC@PC was found to be the best at 25°C with 3.073 mg/g, while adsorption capacity of Rh-B was decreased from 3.070802 mg/g to 2.909148 mg/g with an increasing temperature from 25°C to 45°C.

Effect of pH value: A solution pH also affects the adsorption capacity of adsorbent, so it becomes necessary to study the effect of pH on the process of adsorption. Although varying the range of pH leads to the change of adsorptive molecules and surface assets of adsorbent. The effect of pH on the removal of MG and Rh-B through AC@PC adsorbent performed on different pH values in the range of 2-10 at 25°C temperature, initial dyes concentration 10 mg/L with a dose of adsorbent 3 g/L. To regulate the solution pH, 0.1 N HCl and 0.1 N NaOH was used. It was found that a slight difference in removal percentages were observed at different pH (4, 5, 6, 7, 8, 9 and 10), the highest removal percentage 88.37% (MG) and 92.74% (Rh-B) was observed at pH 7, as shown in Fig. 4(a) and (b). Minimum removal percentage of MG was achieved 86.33% at pH 10 as shown in Fig. 4(a). It was reported that the highest removal of MG dye was observed at 6 pH and minimum adsorption was occurred under acidic condition i.e., at pH 3 (Amiri et al. 2017). Whereas, in this study minimum adsorption percentage of Rh-B was found 89.36% at pH 4 and maximum adsorption takes place at pH 7 (92.7 %) (Fig. 4b). It has been reported in a research that

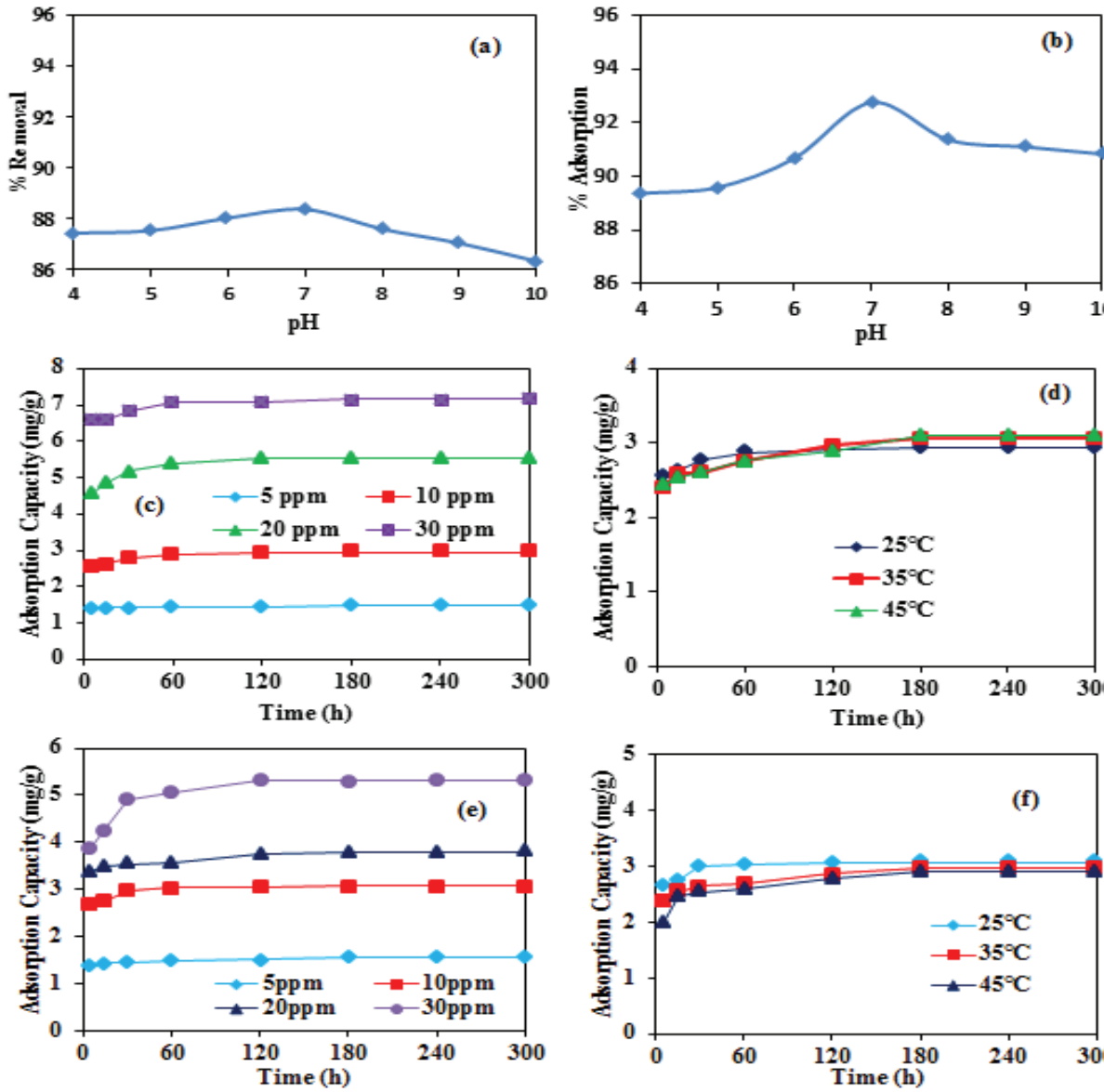

Fig. 4: Effect of pH on adsorption of (a) MG and (b) Rh-B and adsorption capacity of AC@PC for (c) (d) MG and (e) (f) Rh-B at different concentration and temperature respectively.

the maximum removal of Rh-B dye was found at pH 2.1, (Guo et al. 2005) this happen because of the neutralization of OH^- ions present on adsorbent's surface and an increase in the hydrogen ions concentration (Saini et al. 2017). In the present study, the AC@PC adsorbent is of acidic nature, that means hydrogen ions were present on surface of adsorbent whereas both these dyes are cationic dyes with positive charge. At lower pH the H^+ ions concentration on AC@PC was higher that causes the electrostatic repulsion between the adsorbate and adsorbent which is not favourable for dyes removal. At pH 6 and pH 7 the concentration of H^+ ions decreased that protrudes the adsorption through electrostatic attraction, resulting in the neutralization of mixture of adsorbent and adsorbate and shows the maximum removal at neutral pH (Zhang et al. 2016).

Adsorption Isotherms

For optimizing the adsorption design of adsorption system of MG and Rh-B after the effective application of the adsorption techniques it is essential to explain the various adsorption

Table 1: Isotherm parameters for removal of MG and Rh- B by synthesized AC@PC adsorbent.

		MG	Rh-B
Langmuir isotherm	Q_e (mg/g)	9.6246	5.2548
	B (L/mg)	0.3567	0.8855
	RL	0.0854	0.0362
	R^2	0.9929	0.9515
Freundlich Isotherm	K_F (mg/g(L/mg)$^{1/n}$)	2.3624	15.3789
	N	1.7247	1.2450
	R^2	0.9471	0.8602
Temkin Isotherm	B	2.1488	0.8032
	K_T (L/g)	2.21934	1.341635
	R^2	0.9952	0.8602

isotherm models because the adsorption isotherm models undoubtedly describe the correlation between the initial dyes concentration in a solution and amount of dye adsorbed by the adsorbent (Shu et al. 2015). In this work, most commonly known isotherms models were applied for analysing the data obtained through experiments; these models are given as follows: Langmuir, Freundlich and Temkin model of isotherms.

Langmuir isotherm: The Langmuir isotherm model explains that the adsorption happens on homogeneous surface of adsorbent without any interface between adsorbed molecules of dye i.e., monolayer adsorption. For the equilibrium study of MG and Rh-B adsorption, the experiments were performed at different temperatures (25, 35 and 45°**C**) with various initial concentrations of both the dyes (MG and Rh-B) in range of 5-30 mg/L.

The Langmuir isotherm linearly expressed by following equation (Singh et al. 2016):

$$\frac{C_e}{q_e} = \frac{1}{Q_0 \mathrm{b}} + \frac{C_e}{Q_0} \quad \ldots(3)$$

Where,

C_e = Dyes concentration at equilibrium point (mg/L)

q_e = Amount of adsorbate adsorbed at equilibrium (mg/g)

Q_0 = Langmuir constant, maximum capacity of monolayer adsorption (mg/g)

b = rate of adsorption (L/mg)

Linear slope ($1/Q_0$) was obtained after plotting graph of experimental data between C_e/q_e against C_e as shown in the Fig. 5 (a) and (b), the dimensionless separation factor R_L can be expressed by following equation:

$$R_L = \frac{1}{\left(1 + \mathrm{b}C_0\right)} \quad \ldots(4)$$

Where,

C_0 = initial solute concentration (mg/L)

R_L = degree of adsorption

The R_L, separation factor was calculated to check the favourability of adsorption process. The values of R_L, separation factor for the adsorption of MG (Fig. 5a) and Rh-B (Fig. 5b) on the surface of AC@PC adsorbent were occurred in the range of 0.0854-0.359 and 0.0362-0.1842, respectively. Since the R_L values are between 0 and 1, hence is favourable for the adsorption of both MG and Rh-B onto the AC@PC adsorbent surface (Table 1).

Freundlich isotherm: Freundlich isotherm describes the heterogeneous nature of adsorbent. Following equation is used to express the linear form of Freundlich's isotherm model for adsorption process (Hameed and Ahmad, 2009):

$$\ln q_e = \ln K_F + \left(\frac{1}{\mathrm{n}}\right) \ln C_e \quad \ldots(5)$$

Where,

q_e = amount of dyes adsorbed at equilibrium (mg/g)

C_e = concentration of MG and Rh-B at equilibrium point (mg/L)

K_F and n = Freundlich constant, denotes adsorption capacity of AC@PC adsorbent [(mg/g)(L/mg)$^{1/n}$]

The K_F and n values were obtained from the linear slope and intercept of $\ln C_e$ and $\ln q_e$. If the value of 1/n of the slope is between 0 and 1 then it confirms the heterogeneous nature of adsorbent surface and if the values are closer to 0 it shows that the adsorbent surface is highly heterogeneous (Singh et al. 2016). It was observed that the value of Freundlich constant i.e., n for MG and Rh-B dyes was 1.7247 and 1.2450 with R^2 values 0.9471 and 0.8602 respectively as shown in Table 1.

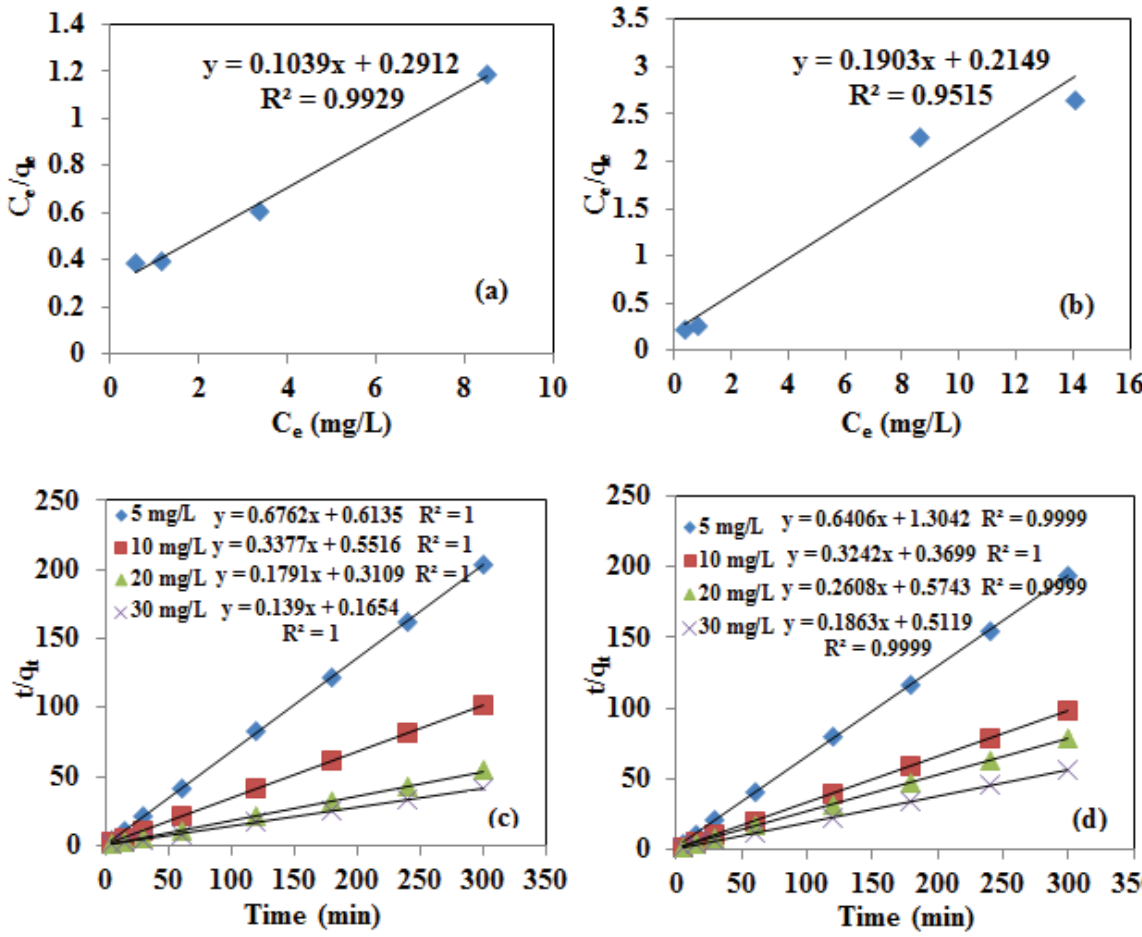

Fig. 5: (a) and (b) Langmuir isotherm plots and (c) and (d) pseudo-second order plots of MG and Rh-B, respectively.

After studying the Langmuir and Freundlich isotherms of adsorption process it was observed that the equilibrium data obtained for MG and Rh-B dyes were best fitted to Langmuir isotherm with R^2 values 0.9929 and 0.9515, respectively that was higher than the R^2 values obtained in Freundlich isotherm.

Temkin isotherm: The linearised graph of Temkin isotherm was obtained by plotting q_e against $\ln C_e$. The K_T value was resolute by slope and intercept of resulted curve. This model undertakes that the heat of absorption that relates with the dye molecules, a function of temperature in the layer would decrease linearly not logarithmically (Chun et al. 2005), as shown in the Eq. 6;

$$q_e = B \ln K_T + B \ln C_e \quad \ldots(6)$$

Where,

B = Temkin constant related to heat of adsorption

K_T = Temkin isotherm equilibrium binding constant

q_e = quantity of dyes adsorbed at equilibrium (mg/g)

C_e = concentration of MG and Rh-B at equilibrium (mg/L)

From the plot of Temkin isotherm the obtained values of $K_T = 2.21934$, $B = 2.1488$, $R^2 = 0.9952$ for MG dye and the values of $K_T = 1.341635$, $B = 0.8032$, $R^2 = 0.8602$ for Rh-B dye.

Kinetic Study

Pseudo-first-order kinetics: Kinetic study involves the analysis of data obtained by experiments using intraparticle diffusion model, pseudo-first-order and pseudo-second-order (Dastkhoon et al. 2017). The kinetics studies were done to comprehend the adsorption process characteristics.

The pseudo-first-order kinetics model is being broadly used to designate the adsorption rate constant in kinetic process (Ho & McKay 1999).

$$\log q_e - q_t = log q_e - \left(\frac{k_1}{2.303}\right) \quad \ldots(6)$$

Where, q_e and q_t denotes the quantity of dyes (MG and Rh-B) in terms of mg/g adsorbed on AC@PC adsorbent at

Table 2: Values of kinetic parameters pseudo first order and second order.

Kinetics			Pseudo first order kinetics			Pseudo second order		
		C_0 (mg/L)	q_e (mg/g)	k_1 (min^{-1})	R^2	q_e (mg/g)	k_2 (g/mg. min)	R^2
AC@PC	MG	5	0.0742	0.002649	0.9103	1.4788	0.7453	1
		10	0.3629	0.004082	0.9877	2.9612	0.2067	1
		20	0.7120	0.003474	0.8811	5.5834	0.1031	1
		30	0.7120	0.003561	0.7857	7.1942	0.1168	1
	Rh-B	5	0.2123	0.003865	0.9050	1.5610	0.3146	0.999
		10	0.3202	0.004993	0.8417	3.0845	0.2841	1
		20	0.4530	0.002996	0.9475	3.8343	0.1184	0.999
		30	1.0690	0.004386	0.9583	5.3676	0.0678	0.999

time t (min) at equilibrium point. K_1 (min^{-1}) represents rate constant for the MG and Rh-B adsorption. Values of k_1 and q_e were obtained by calculating $\log(q_e\text{-}q_t)$ against t plots with different dyes initial concentrations of MG and Rh-B. It was observed that adsorption data was not fitted with pseudo-first order with R^2 value = 0.785-0.910 for MG and R^2 value = 0.841-0.958 for Rh-B (Table 2).

Pseudo-second-order kinetics: The experimental records were examined by using pseudo-second-order kinetics (Li et al. 2013). The equation for pseudo-second-order kinetics is expressed below:

$$\frac{t}{qt} = \frac{1}{\left(k_2 q_e^2\right)} + \left(\frac{1}{q_e}\right)t \qquad \ldots(8)$$

Here, k_2 (g/(mg.min) is constant for pseudo second order kinetic. q_e denotes the adsorption capacity at equilibrium.

Values of pseudo second order kinetic parameters were calculated from the plot of t/q_t against t (Figs. 5c and d). The linear regression coefficient (R^2) values for both the kinetic models are given in Table 3. The pseudo second order model was best fitted with kinetic data with R^2 value =1 for MG (Fig. 5c) and R^2 value = 0.999 for Rh-B (Fig. 5d).

Intraparticle diffusion model: An experimental model for intraparticle diffusion mechanism, reported by Albadarin et al. (2017) was used. The solute transfer in process of solid-liquid sorption is commonly illustrated by intraparticle diffusion model. Intraparticle diffusion model is represented by following equation:

$$q_t = k_i t^{1/2} + c \qquad \ldots(9)$$

Here, k_i (mg/g.min$^{1/2}$) symbolizes the rate constant for intraparticle diffusion and constant C (mg/g) is associated with the boundary layer and was calculated through graph plotted between q_t and $t^{1/2}$. Intraparticle diffusion model is a rate limiting step. The intraparticle diffusion is consider as rate limiting step when a linear regression passage origin is found after plotting the graph between q_t and $t^{1/2}$. Fig. 6 shows that the plots did not passed through the origin in case of both the dyes (MG (Fig. 6a) and Rh-B (Fig. 6b)). This signifies that the intraparticle diffusion model was not only the rate controlling factor and other mechanisms are also involved (Saleh et al. 2016).

Thermodynamic Study

Thermodynamic study includes calculation of Gibb's free energy (ΔG°), change in entropy (ΔS) and enthalpy (ΔH) from the following equations for adsorption of MG and Rh-B dyes (Singh et al. 2016)

$$\mathrm{Kc} = \frac{qe}{Ce} \qquad \ldots(10)$$

$$\ln \mathrm{Kc} = \frac{\Delta S}{R} - \frac{\Delta \mathrm{H}}{RT} \qquad \ldots(11)$$

$$\Delta G^\circ = -RT\,Ln\,Kc \qquad \ldots(12)$$

Where, C_e is the concentration of the dye (mg/L) in the solution and q_e is the amount of dye adsorbed at equilibrium (mg/g), T(K) is the absolute temperature and K_c is the thermodynamic equilibrium constant.

The standard Gibb's energy (ΔG°) was calculated by the value of K_c (L/g) obtained at different temperatures and R is the universal gas constant (8.314 J/mol K). The values of thermodynamic constants were calculated by graph of $\ln K_c$ plotted against 1/T. The thermodynamic data shows that the MG dye (Fig. 6c) adsorption by AC@PC adsorbent was endothermic that was proved by the positive value of ΔH° (22.51348 J/mol) (Table 3), whereas spontaneous nature of adsorption process which is favourable at all temperatures described by negative value of ΔG° (Mahmoodi et al. 2011). The standard entropy i.e., ΔS° (83.15663 J/mol K) for MG

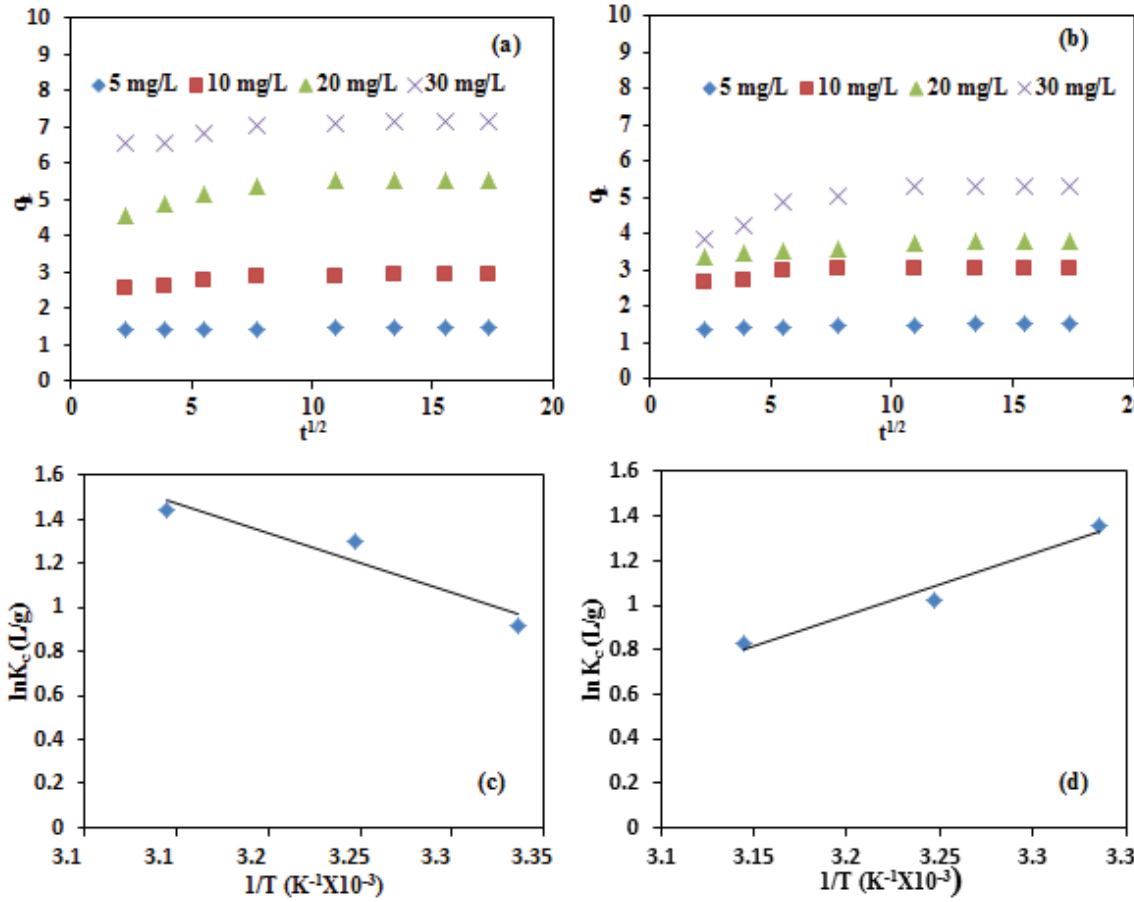

Fig. 6: (a) and (b) Intraparticle diffusion model and (c) and (d) thermodynamics plot of MG and Rh-B, respectively.

Table 3: Thermodynamic parameters of MG and Rh-B adsorption onto AC@PC adsorbent.

Parameters	Temperature (K)	AC@PC	
		MG	Rh-B
ΔG° (KJ/mol)	298	-24.7582	19.64981
	308	-25.5897	20.30998
	318	-26.4213	20.97014
ΔH° (J/mol)		22.51348	-23.10210
ΔS° (J/mol K)		83.15663	-66.01648

adsorption was positive, it represents that the degree of adsorbent-adsorbate interface randomness during adsorption process of dye. However, in case of Rh-B (Fig. 6d) value of ΔG° was positive. The negative values -23.10210 J/mol and -66.01648 J/mol K of ΔH° and ΔS°, respectively, (Table 3) confirmed that the thermodynamic process was exothermic, on increasing temperature the initial adsorption rate was decreased. It was examined that the value of ΔG° increases with increasing temperature which indicates greater adsorption at lower temperature. For Rh-B negative value of ΔS° revealed good affinity of AC@PC. Analogous result was also reported by Shu et al. (2015). This study explained that adsorption of Rh-B onto the adsorbate (rice husk and activated carbon) was exothermic in nature with negative values of ΔH° and ΔS°.

Mechanism

Mechanism of dyes adsorption can be described by various

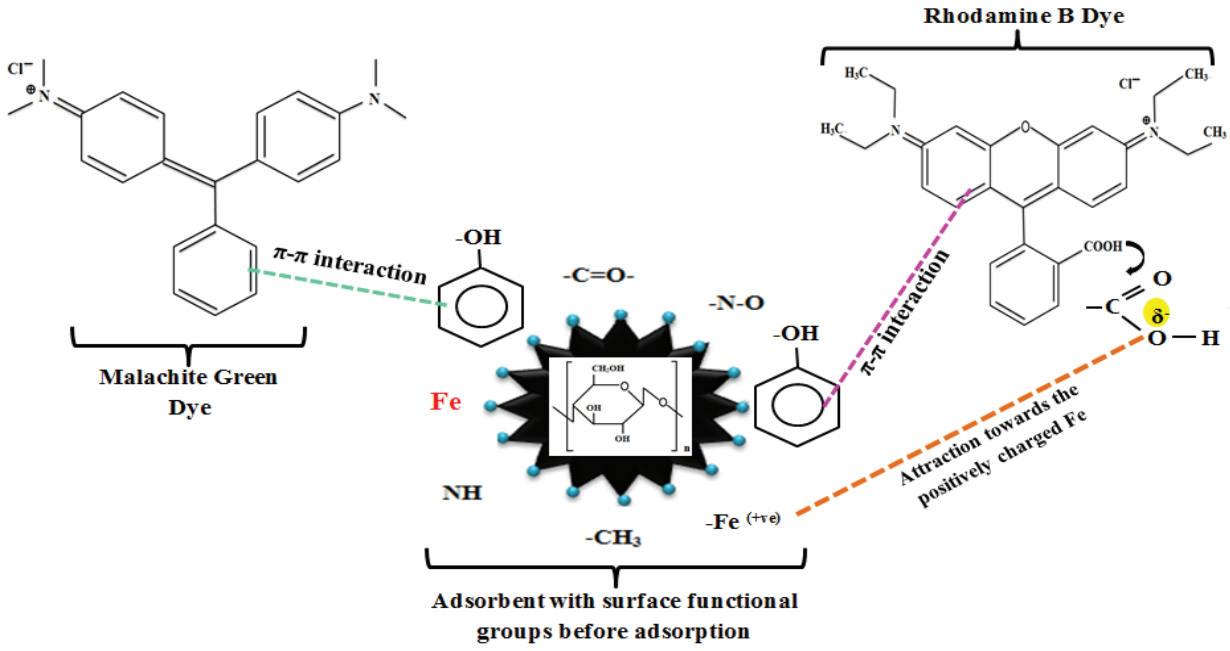

Fig. 7: Mechanism of dyes adsorption on AC@PC.

processes. In this study, Langmuir isotherm was best fitted. The Langmuir isotherm signifies the monolayer adsorption onto a determinate number of homogeneous sites. The homogeneous nature of adsorption phenomenon can also be explained by FTIR results that represent the functional groups are present on the surface of adsorbent that may be responsible for enhancing the removal percentage of adsorbent. As shown in Fig. 7, FTIR results revealed the presence of several functional groups like hydroxyl, phenol, carboxylic acid, benzene ring, amine, methyl, and nitro group on the surface of adsorbent before adsorption of dyes. But after adsorption of dyes, some changes were also observed in the functional group composition. In case of MG, -NH, -CH, and C=H groups are mainly responsible groups for adsorption of dye. Whereas, in case of Rh-B adsorbent, after adsorption shows that OH, -CH, -C=O, -C-O and N-C=O functional groups had key role in removal. FTIR result revealed the possibility of ion exchange of dyes on adsorbent surface and helps to increase the adsorption percentage and provide more active binding sites for adsorption of dyes. Elemental analysis was done by EDS that shows that higher carbon content was present in adsorbent that provides large surface area to the adsorbent; more the surface area more the adsorption of dyes.

The adsorption of organic dyes onto the surface of activated carbon in this study can be explained on the basis of mainly two major mechanisms i.e., electrostatic attraction and p-p interaction. The electrostatic attraction mechanism undertakes the attraction of partially negative species towards the positively charged species, as the surface functional group (Fe) on adsorbent acts as an electron acceptor while Rh-B dye has a partially negatively charged group that attracted towards the Fe present on the adsorbent surface with positive charge. On the other hand, p-p interaction, takes place in between the benzene ring present in adsorbate and on adsorbent surface. Adsorption of MG and Rh-B through AC@PC was occurred by p-p interaction a similar mechanism was also reported by Gao et al. 2019 (MG) and Cheng et al. 2017 (Rh-B).

CONCLUSIONS

A simple and cost-effective method to synthesize adsorbent from waste disposable cups at 500°C temperature in muffle furnace and then used for removal of MG and (Rh-B) dyes from an aqueous solution. AC@PC is low cost and easily available material. Prepared AC@PC adsorbent showed excellent removal ability for MG and Rh-B dyes. The adsorption behaviour of MG and Rh-B was analysed methodically and observed that pseudo-second-order kinetic with the $R^2 > 0.999$ was followed by both the dyes. The Langmuir model of isotherm was best fitted to the experimental data of equilibrium study. It can be concluded that disposable waste cups can be effectively used for the synthesis of adsorbent which is cost effective and the synthesized adsorbent AC@PC from waste paper cups could be used to remove effectively the basic dyes from dye contaminated water. An application of waste cups in water

treatment not only treats water but also minimize the waste generation.

ACKNOWLEDGMENT

The authors are very grateful to acknowledge the support of UGC-BSR research start-up-grant (Project No. F. 30-382/2017, BSR) and Science and Engineering Research Board (SERB), Department of Science and Technology (DST) (Reference no. ECR/2016/001924), Government of India.

REFERENCES

Albadarin, A.B., Collins, M.N., Naushad, M., Shirazian, S., Walker, G. and Mangwandi, C. 2017. Activated lignin-chitosan extruded blends for efficient adsorption of methylene blue. Chem. Eng. J., 307: 264-272.

Amiri, M., Niasari, M.S., Akbari, A. and Gholami, T. 2017. Removal of malachite green (a toxic dye) from water by cobalt ferrite silica magnetic nanocomposite: Herbal and green sol-gel autocombustion synthesis. Int. J. Hydrog. Energy., 42(39): 24846-24860.

Arena, U., Ardolino, F. and Gregorio F.D. 2016. Technological, environmental and social aspects of a recycling process of post-consumer absorbent hygiene products. J. Clean. Prod., 127: 289-301.

Arumugam, K., Ganesan, S., Muthunarayanan, V., Vivek, S., Sugumar, S. and Munusamy, V. 2015. Potentiality of *Eisenia fetida* to degrade disposable paper cups-an ecofriendly solution to solid waste pollution. Environ. Sci. Pollut. Res., 22(4): 2868-2876.

Arumugam, K., Renganathan, S., Babalola, O.O. and Muthunarayanan, V. 2018. Investigation on paper cup waste degradation by bacterial consortium and Eudrillus eugeinea through vermicomposting. Waste Manage., 74: 185-193.

Bhattacharya, K., Gupta, S. and Sharma, G. 2014. Interactions of the dye, rhodamine-B with kaolinite and montmorillonite in water. Appl. Clay. Sci., 99: 7-17.

Chun, J.H., Jeon, S.K., Kim, N.Y. and Chun, J.Y. 2005. The phase shift method for determining Langmuir and Temkin adsorption isotherms of over potentially deposited hydrogen for the cathodic H_2 evaluation reaction at the poly-Pt/H_2SO_4 aqueous electrolyte interface. Int. J. Hydrog. Energy., 30(13-14): 1423-1436.

Cheng, Z.L., Li, Y.X. and Liu, Z. 2017. Novel adsorption materials based on graphene oxide/Beta zeolite composite materials and their adsorption performance for rhodamine B. J. Alloys. Compd., 708: 255-263.

Crini, G. 2006. Non-conventional low-cost adsorbents for dye removal: A review. Bioresour. Technol., 97(9): 1061-1085.

Dastkhoon, M., Ghaedi, M., Asfaram, A., Azqhandi, M.H.A. and Purkait, M.K. 2017. Simultaneous removal of dyes onto nanowires adsorbent use of ultrasound assisted adsorption to clean waste water: Chemometrics for modeling and optimization, multicomponent adsorption and kinetic study. Chem. Eng. Res. Des., 124: 222-237.

Gao, M., Wang, Z., Yang, C., Ning, J., Zhou, Z and Li, G. 2019. Novel magnetic graphene oxide decorated with persimmon tannins for efficient adsorption of malachite green from aqueous solutions. Colloids Surf. A Physicochem. Eng. Asp., 566: 48-57.

Gautam, A., Rawat, S., Verma, L., Singh, J., Sikarwar, S., Yadav, B.C. and Kalamdhad, A.S. 2018. Green synthesis of iron nanoparticle from extract of waste tea: An application for phenol red removal from aqueous solution. Environ. Nanotechnol. Monit. Manage., 10: 377-387.

Guo, Y., Zhao, J., Zhang, H., Yang, S., Qi, J., Wang, Z. and Xu, H. 2005. Use of rice husk-based porous carbon for adsorption of Rhodamine B from aqueous solutions. Dyes Pigm., 66(2): 123-128.

Gupta, N., Kushwaha, A.K. and Chattopadhyaya, M.C. 2016. Application of potato (*Solanum tuberosum*) plant wastes for the removal of methylene blue and malachite green dye from aqueous solution. Arab. J. Chem., 9: 707-716.

Gupta, V.K., Pathania, D., Agarwal, S. and Singh, P. 2012. Adsorptional photocatalytic degradation of methylene blue onto pectin-CuS nanocomposite under solar light. J. Hazard. Mater., 243: 179-186.

Hameed, B.H. and Ahmad, A.A. 2009. Batch adsorption of methylene blue from aqueous solution by garlic peel, an agricultural waste biomass. J. Hazard. Mater., 164(2-3): 870-875.

Ho, Y.S. and McKay, G. 1999. Pseudo-second order model for sorption processes. Process Biochem., 34(5): 451-465.

Ibrahim, M., Siddiqe, A., Verma, L., Singh, J. and Koduru, J.R. 2019. Adsorptive removal of fluoride from aqueous solution by biogenic iron permeated activated carbon derived from sweet lime waste. Acta Chim. Slov., 66(1): 123-136.

Kant, R. 2012. Adsorption of dye eosin from an aqueous solution on two different samples of activated carbon by static batch method. J. Water Resource Prot., 4(02): 93-98.

Karunanayake, A., Todd, O.A., Crowely, M., Ricchetti, L., Pittman, Jr C.U., Anderson, R., Mohan, D. and Mlsna, T. 2018. Lead and cadmium remediation using magnetized and nonmagnetized biochar from Douglas fir. Chem. Eng. J., 331: 480-491.

Kono, H. 2015. Preparation and characterization of amphoteric cellulose hydrogels as adsorbents for the anionic dyes in aqueous solutions. Gels., 1(1): 94-116

Li, Y.H., Du, Q.J., Liu, T.H., Sun, J.K., Wang, Y.H., Wu, S.L., Wang, Z.H., Xia, Y.Z. and Xia, L.H. 2013. Methylene blue adsorption ongraphene oxide/calcium alginate composites. Carbohydr. Polym., 95(1): 501-507.

Lunge, S., Singh, S. and Sinha, A. 2014. Magnetic iron oxide (Fe_3O_4) nano- particles from tea waste for arsenic removal. J. Magn. Magn. Mater. 356: 21-31.

Magdalane, C.M., Kaviyarasu, K., Vijaya, J.J., Jayakumar, C., Maaza, M. and Jeyaraj, B. 2017. Photocatalytic degradation effect of malachite green and catalytic hydrogenation by UV illuminated CeO2/CdO multilayered nanoplatelet arrays: Investigation of antifungal and antimicrobial activities. J. Photochem. Photobiol. B., 169: 110-123.

Mahmoodi, N., Hayati, M.B., Arami, M. and Lan, C. 2011. Adsorption of textile dyes on pine cone from colored wastewater: kinetic, equilibrium and thermodynamic studies. Desalination, 268(1-3): 117-125.

Nassar, M.Y., Mohamed, T.Y., Ahmed, I.S. and Sami, I. 2017. MgO nanostructure via a sol-gel combustion synthesis method using different fuels: An efficient nano-adsorbent for the removal of some anionic textile dyes. J. Mol. Liq., 225: 730-740.

Ngulube, T., Gumbo, J.R., Masindi, V. and Maity, A. 2017. An update on synthetic dyes adsorption onto clay based minerals: A state-of-art review. J. Environ. Manage., 191: 35-57.

Noel, D.S. and Rajan, M.R. 2014. Impact of dyeing industry effluent on groundwater quality by water quality index and correlation analysis. J. Pollut. Eff. Control., 2: 1-4.

Pathania, D., Sharma, S. and Singh, P. 2017. Removal of methylene blue by adsorption onto activated carbon developed from Ficus carica bast. Arab. J. Chem., 10: 1445-1451.

Saini, J., Garg, V.K. and Kataria, N. 2017. Removal of Orange G and Rhodamine B dyes from aqueous system using hydrothermally synthesized zinc oxide loaded activated carbon (ZnO-AC). J. Environ. Chem. Eng., 5(1): 884-892.

Saleh, T.A., Siddiqui, M.N. and Al-Arfaj, A.A. 2016. Kinetic and intraparticle diffusion studies of carbon nanotubes-titania for desulfurization of fuels. Petrol. Sci. Technol., 34(16): 1468-1474.

Salleh, M.A.M., Mahmoud, D.K., Karim, W.A. and Idris, A. 2011. Cationic anionic dye adsorption by agricultural solid waste: a comprehensive review. Desalination, 280(1-3): 1-13.

Sartape, A.S., Mandhare, A.M., Jadhav, V.V., Raut, P.D., Anuse, M.A. and Kolekar, S.S. 2017. Removal of malachite green dye from aqueous solution with adsorption technique using *Limonia acidissima* (wood apple) shell as low cost adsorbent. Arab J. Chem., 10: 3229-3238.

Shu, J., Wang, Z., Huang, Y., Huang, N., Ren, C. and Zhang, W. 2015. Adsorption removal of Congo red from aqueous solution by polyhedral Cu2O nanoparticles: Kinetics, isotherms, thermodynamics and mechanism analysis. J. Alloys Compd., 633: 338-346.

Singh, J. and Lee, B.K. 2015. Hydrometallurgical recovery of heavy metals from low grade automobile shredder residue (ASR): an application of advance Fenton process (AFP). J. Environ. Manage., 161: 1-10.

Singh, J., Reddy, K.J., Chang, Y.Y., Kang, S.H. and Yang, J.K. 2016. A novel reutilization method for automobile shredder residue as an adsorbent for the removal of methylene blue: Mechanisms and heavy metal recovery using an ultrasonically assisted acid. Process Saf. Environ., 99: 88-97.

Yagub, M.T., Sen, T.K., Afroze, S. and Ang, H.M. 2014. Dye and its removal from aqueous solution by adsorption: A review. Adv. Colloid Interface Sci., 209: 172-184.

Zhang, F., Ma, B.L., Jiang, X.P. and Ji, Y.F. 2016. Dual function magnetic hydroxyapatite nano powder for removal of malachite green and Congo red from aqueous solution. Powder Technol., 302: 207-214.